Quantum Electronics **43** (2) 167–173 (2013)

OPTICAL FIBRES

PACS numbers: 42.81.Cn; 42.81.Dp; 42.81.Gs
DOI: 10.1070/QE2013v043n02ABEH014952

Propagation of broadband optical radiation in a spun high-birefringent fibre

Ya.V. Przhiyalkovsky, S.K. Morshnev, N.I. Starostin, V.P. Gubin

Abstract. **The evolution of the polarisation state of the broadband optical radiation, propagating through a spun high-birefringent fibre is studied. A theoretical model describing the polarisation state of the radiation in the spun fibre depending on the input polarisation parameters is developed. The model is based on the geometric analysis of the polarisation states of the spectral components of the radiation on the Poincare sphere. It is shown that when the propagation path length of the radiation in the optical fibre exceeds some value (the coherence length), the spectrum-averaged polarisation state of the output light is determined only by the parameters of the spun fibre, while the degree of polarisation of the output radiation depends on the input polarisation state.**

Keywords: *optical fibre, spun fibre, polarisation of radiation.*

1. Introduction

Optical spun fibre was proposed in 1989 [1] as a sensitive element for an electric current and magnetic field sensor on the base of Faraday magnetooptical effect [2–4]. Spun fibre is fabricated by drawing from a rotating preform with strong built-in linear birefringence (BR). Due to the helix structure of the built-in linear BR axes [5] in spun fibres, a compromise is achieved between the high magnetooptical sensitivity and its stability with respect to fibre deformations, e.g., bending [1, 5–7]. Theoretical analysis shows that to suppress the influence of bending-induced linear BR on the fibre sensitivity, the built-in linear BR of the helix structure should be 30 times greater [5]. Thus, for dealing with loops less than 5 mm in diameter the required beat length of the built-in BR should not exceed 1 mm [6]. Such parameters can be provided by microstructure spun fibres [8–10]. However, the pitch of the helix structure, required to suppress the already built-in linear BR and make the Faraday effect observable, is usually technologically limited from below at the level of 2–3 mm. Under such conditions the polarisation states (PS) of light, propagating along the spun fibre, may evolve via the states having the ellipticity, rather far from that of circular PS [8].

This gives rise to a number of problems, when using the microstructure spun fibres in a reciprocal reflective interferometer [2] of a current sensor. One of these problems is the reduction of the informative component of light under reflection from the interferometer mirror, since the reflection does not transform the elliptic PS into an orthogonal elliptic state (as it occurs, e.g., with circular PS). As a result the contrast (the visibility of interference pattern) of the interferometer is reduced [8], which leads to the reduction of the dynamic range of the electric current sensor.

It is known (see, e.g., [1]) that in order to increase the accuracy of electric current measurements with a reflective interferometer it is necessary to use relatively broadband sources of optical radiation. Thus, near 1.55 μm the spectral width of the sources amounts to 20–25 nm. Therefore, in the studies of factors affecting the contrast, it is important to take the nonmonochromaticity of the source radiation into account. However, currently in the literature the PS evolution in a spun fibre is thoroughly considered only for monochromatic radiation [5, 7, 11]; while the influence of the spectral width, as a rule, is taken into account only phenomenologically. Worth noting is paper [12], in which the theory is developed to describe the coupling of orthogonal polarisation modes of optical radiation, caused by random torsions in a polarisation-maintaining optical waveguide. In principle, this theory removes the limitations, imposed on the fibre parameters and the spectral characteristics of the source in numerical calculations of the light PS evolution in a long fibre, but the analysis of spun waveguides using this theory was not carried out.

Another problem that requires a detailed study is depolarisation of broadband light in a spun fibre of sufficiently large length and its dependence on the input polarisation. The study of depolarisation of linear polarised light in a spun fibre, carried out in [13], has shown that the residual polarisation of light at the output of a long segment of the fibre does not depend on the input polarisation; however, the details of this process are studied insufficiently.

The aim of the present paper is to investigate theoretically and experimentally the evolution of spectrally averaged PSs of broadband light during its propagation through a spun fibre with strong built-in BR.

2. Theory

2.1. Fundamentals of theoretical analysis of spun fibres

The description of polarisation parameters of light waves, propagating in optical fibres, often uses the formalism of differential Jones matrices. The evolution of the Jones vector, characterising the PS of light radiation, in this case may be described by the differential equation

$$\frac{d\boldsymbol{E}}{dz} = N\boldsymbol{E}, \qquad (1)$$

Ya.V. Przhiyalkovsky, S.K. Morshnev, N.I. Starostin, V.P. Gubin
V.A. Kotel'nikov Institute of Radio Engineering and Electronics, Fryazino Branch, Russian Academy of Sciences, pl. Vvedenskogo 1, 141120 Fryazino, Moscow region, Russia; 'Profotech' CJSC, office 613, Vereyskaya ul. 17 (Vereyskaya Plaza), 121357 Moscow, Russia
e-mail: yankus.p@gmail.com, nis229@ire216.msk.su

Received 13 August 2012
Kvantovaya Elektronika **43** (2) 167–173 (2013)
Translated by V.L. Derbov

where $\boldsymbol{E}$ is the Jones vector, consisting of complex amplitudes of the components of the wave electric field strength and N is the differential Jones matrix of the optical fibre.

The differential Jones matrix for a rectilinear segment of a spun fibre in the basis of the circular PS is expressed as [5]

$$N_{\rm c}(z) = \begin{pmatrix} \mathrm{i}\dfrac{\gamma}{2} & \mathrm{i}\dfrac{\Delta\beta}{2}\exp(-\mathrm{i}2\xi z) \\ \mathrm{i}\dfrac{\Delta\beta}{2}\exp(\mathrm{i}2\xi z) & -\mathrm{i}\dfrac{\gamma}{2} \end{pmatrix}, \quad (2)$$

where γ is the growth rate of phase delay between the waves with orthogonal circular polarisations due to Faraday effect; $\Delta\beta = k_y - k_x = 2\pi/L_{\rm b}$ is the growth rate of phase delay between the waves with orthogonal linear polarisations, determined by the built-in linear BR with the beat length $L_{\rm b}$; $\xi = 2\pi/L_{\rm tw}$ is the frequency of spatial rotation of the axes of built-in linear BR with the helix pitch $L_{\rm tw}$; and z is the coordinate along the fibre axis.

To describe the PS of radiation, it is convenient to use the formalism of its representation on the complex plane [14]. Each point of this plane corresponds to a complex number, which is a ratio of the Jones vector components. In the basis of circular polarisations, in which E_r and E_l are the Jones vector components, the polarisation state is represented by the point $\chi_{\rm c} = E_l/E_r$ of the complex plane. The zero of the coordinate system of the complex plane and the infinity correspond to the basis polarisation states.

A one-to-one correspondence exists between the points of the plane and the points of the sphere, to which this plane is tangent (the Poincare sphere) [14, 15]. The basis polarisation states on the Poincare sphere are located at the tangency point and the antipode one. In the basis of circular polarisation the south pole of the Poincare sphere represents the left-hand circular PS, while the north pole represents the right-hand circular PS, and at the equator the linear PS with different azimuths are mapped. The circles of equal latitude, parallel to the equator, represent the variety of the PSs with equal ellipticity, while the arcs of equal longitude correspond to the PSs with equal azimuths.

It is known that the transformation from the circular PS coordinate system to an arbitrary elliptical PS coordinate system can be implemented by two rotations of the Poincare sphere: first, by the angle α about the axis, connecting the points of the circular PS, and, second, by the angle φ about the axis, connecting two points of the orthogonal linear PS with the azimuths $\pm\pi/4$ [16] (see Fig. 1). The final transformation matrix is a product of the appropriate rotation matrices and has the form

$$T = T(\varphi,\alpha) = T_2(\varphi)T_1(\alpha)$$

$$= \begin{pmatrix} \exp\left(\mathrm{i}\dfrac{\alpha}{2}\right)\cos\dfrac{\varphi}{2} & \exp\left(-\mathrm{i}\dfrac{\alpha}{2}\right)\sin\dfrac{\varphi}{2} \\ -\exp\left(\mathrm{i}\dfrac{\alpha}{2}\right)\sin\dfrac{\varphi}{2} & \exp\left(-\mathrm{i}\dfrac{\alpha}{2}\right)\cos\dfrac{\varphi}{2} \end{pmatrix}. \quad (3)$$

In the new coordinate system with the Jones vector components E_u and E_v the representation of the PS on the complex plane will be determined by the number $\chi_{\rm e} = E_v/E_u$. On the Poincare sphere, built on this plane, the basis PS are again located at the poles; however, in the new coordinate system they are elliptical.

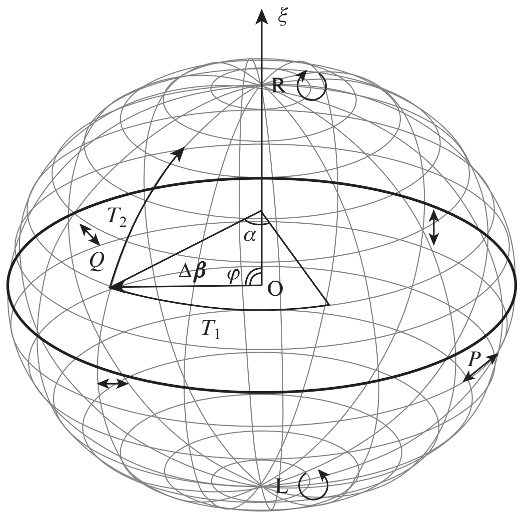

Figure 1. Motion of PS points on the Poincare sphere as a result of transformation to the rotating system of coordinates.

2.2. Evolution of polarisation of monochromatic light in a spun fibre, described in the rotating reference frame

Let us study the PS evolution of the monochromatic light radiation in a spun fibre. It is convenient to consider the transformation of complex amplitudes of the electric field vector in the helical coordinate system, accompanying the axes of the built-in linear BR of the spun fibre. In the space of the PS, mapped by points on the Poincare sphere, we will refer to it as the rotating coordinate system.

Let the slow axis of the built-in linear BR of the spun fibre be horizontal at the initial point. In this case on the Poincare sphere the BR vector is directed towards the horizontal linear PS. Let us perform the transformation from the laboratory system of circular PS coordinates to the one, rotating with the frequency 2ξ, by substituting the angle $\alpha = \alpha(z) = -2\xi z$ and a certain angle $0 \leqslant \varphi \leqslant \pi/2$ into the transition matrix (3) (Fig.1). From the dependence $\alpha(z)$ of the angle of rotation about the vertical axis, which is the axis of rotation of the linear BR vector, it is seen that the new coordinate system rotates with respect to the laboratory one together with the vector of the built-in linear BR with the frequency of its rotation 2ξ. The evolution equation for the electric field vector (1) with Eqn (3) taken into account has the form:

$$\frac{\mathrm{d}}{\mathrm{d}z}\begin{pmatrix} E_u \\ E_v \end{pmatrix} = \frac{\mathrm{d}}{\mathrm{d}z}\left(T\begin{pmatrix} E_r \\ E_l \end{pmatrix}\right) = \left(\frac{\mathrm{d}T}{\mathrm{d}z}T^{-1} + TN_{\rm c}T^{-1}\right)\begin{pmatrix} E_u \\ E_v \end{pmatrix}. \quad (4)$$

Performing the matrix multiplication, we arrive at the equations describing the Jones vector variation in the new coordinate system:

$$\begin{pmatrix} \mathrm{d}E_u/\mathrm{d}z \\ \mathrm{d}E_v/\mathrm{d}z \end{pmatrix} = \left[\mathrm{i}\left(\xi + \frac{\gamma}{2}\right)\begin{pmatrix} \cos\varphi & -\sin\varphi \\ -\sin\varphi & -\cos\varphi \end{pmatrix}\right.$$

$$\left. + \mathrm{i}\frac{\Delta\beta}{2}\begin{pmatrix} \sin\varphi & -\cos\varphi \\ -\cos\varphi & -\sin\varphi \end{pmatrix}\right]\begin{pmatrix} E_u \\ E_v \end{pmatrix}. \quad (5)$$

From Eqn (5) it follows that if the angle φ is taken such that

$$\tan\varphi = \frac{\Delta\beta}{2\xi+\gamma}, \tag{6}$$

then the PS evolution equation in the rotating coordinate system of the elliptical PS can be expressed in the simple form:

$$\begin{pmatrix} \mathrm{d}E_u/\mathrm{d}z \\ \mathrm{d}E_v/\mathrm{d}z \end{pmatrix} = \mathrm{i}\frac{\Omega}{2}\begin{pmatrix} 1 & 0 \\ 0 & -1 \end{pmatrix}\begin{pmatrix} E_u \\ E_v \end{pmatrix} = N_\mathrm{e}\begin{pmatrix} E_u \\ E_v \end{pmatrix}, \tag{7}$$

where

$$\Omega = (2\xi+\gamma)\left[1+\left(\frac{\Delta\beta}{2\xi+\gamma}\right)^2\right]^{1/2}. \tag{8}$$

By integrating Eqn (7) we obtain the Jones matrix for a rectilinear spun fibre in the rotating coordinate frame

$$\begin{pmatrix} E_u(z) \\ E_v(z) \end{pmatrix} = \begin{pmatrix} \exp\left(\mathrm{i}\frac{\Omega}{2}z\right) & 0 \\ 0 & \exp\left(-\mathrm{i}\frac{\Omega}{2}z\right) \end{pmatrix}\begin{pmatrix} E_u(0) \\ E_v(0) \end{pmatrix}. \tag{9}$$

In the complex plane the polarisation state is expressed by the variable

$$\chi_\mathrm{e}(z) = \frac{E_v(z)}{E_u(z)} = \chi_\mathrm{e}(0)\exp(-\mathrm{i}\Omega z). \tag{10}$$

Equation (10) describes the motion of the PS point in the complex plane in the rotating coordinate frame of the elliptic PS along the circle, having the radius $|\chi_\mathrm{e}(0)|$, with the frequency Ω and the centre at the zero point, corresponding to one of the basis PS of the rotating coordinate frame.

From the character of the transformation to the rotating coordinate system of the elliptic PS it is seen that the points of its basis PS lie on the Poincare sphere in the plane, containing the vector of built-in linear BR and the axis of its rotation. In the laboratory system of the circular PS these points rotate on the Poincare sphere together with the vector of the built-in linear BR about the axis of its rotation with the frequency 2ξ at the constant latitudes $\psi = \pm(\pi/2 - \varphi)$, where φ is determined by the parameters of the fibre, entering Eqn (6). The axis, passing through the points of the basis PS of the rotating coordinate system, may be called the instantaneous axis. Hence, in the laboratory system of coordinates the motion of the PS point is a combination of two rotations, namely, the PS point rotates with the frequency Ω about the instantaneous axis, which, in turn, rotates with the frequency 2ξ of the built-in BR rotation about the axis, connecting the points of the circular PS. Note, that the spatial frequency of rotation Ω is equal to twice the frequency, defined in Ref. [13], which is due exclusively to the difference in definitions.

The pitch of the helix of the axes of built-in linear BR $L_\mathrm{tw} = 2\pi/\xi$ usually amounts to a few millimetres. In comparison with it, the beat length of circular BR, introduced by the Faraday effect, $L_\mathrm{F} = 2\pi/\gamma$ in practice is sufficiently large, i.e., $\gamma \ll \xi$. Therefore

$$\tan\varphi = \frac{\Delta\beta}{2\xi+\gamma} \approx \frac{\Delta\beta}{2\xi} = \frac{L_\mathrm{tw}}{2L_\mathrm{b}} = \sigma. \tag{11}$$

The ratio of the helix pitch to the doubled beat length of the built-in BR, denoted by σ, is a parameter, important for further analysis of spun fibres.

2.3. Propagation of broadband light in spun fibres

Consider the propagation of radiation with broad spectrum through a spun fibre. All formulae of Section 2.2 keep valid for each wavelength that determines the spectrum of light entering the fibre. However, now one should take into account that the Verdet constant [17], to which the circular BR induced due to the Faraday effect is proportional, as well as the built-in linear BR, become dependent on the wavelength. Since, as mentioned above, $\gamma \ll \xi$, and these two quantities enter all expressions in the form of a sum, the dependence of γ on the wavelength can be neglected with high accuracy. The beat length of the built-in linear BR is proportional to the wavelength of light [8] $L_\mathrm{b}(\lambda) \sim \lambda$. In this case the angle φ, by which we rotate the Poincare sphere performing the transformation to the rotating coordinate system of the elliptical PS [see Eqn (6)], is, in turn, a function of the wavelength. Consider a rectangular radiation spectrum with the centre wavelength $\lambda_0 = 1550$ nm and the width $\Delta\lambda = 20$ nm. Let $L_\mathrm{b}(\lambda_0) = 2\pi/\Delta\beta(\lambda_0) = 1.7$ mm; $L_\mathrm{tw} = 2.68$ mm; then the angle φ varies from $\varphi_\mathrm{min} = \varphi(\lambda = 1540\ \mathrm{nm}) = 37.86°$ to $\varphi_\mathrm{max} = \varphi(\lambda = 1560\ \mathrm{nm}) = 38.22°$. Thus, the angle φ very weakly depends on the wavelength, and in the first approximation it may be treated as constant $\varphi = \varphi(\lambda_0)$.

Consider the evolution of polarisations of individual spectral components of the broadband radiation on the complex plane in the rotating coordinate system of the elliptical PS. The complex variable of the polarisation state becomes a function of the wavelength:

$$\chi_\mathrm{e}(\lambda, z) = \chi_\mathrm{e}(0)\exp[-\mathrm{i}\Omega(\lambda)z]$$
$$= \chi_\mathrm{e}(0)\exp\left\{-\mathrm{i}(2\xi+\gamma)\left[1+\left(\frac{\Delta\beta(\lambda)}{2\xi+\gamma}\right)^2\right]^{1/2} z\right\}. \tag{12}$$

From Eqn (12) it is seen that the PS point rotation frequency for each spectral component about the origin of coordinates depends on its wavelength. At the fibre input the PS of all components are similar and equal to the initial one. As the radiation propagates along the fibre, the set of PS points of the spectral components spreads from one point onto an arc of the circle of the radius $|\chi_\mathrm{e}(0)|$, the length of which increases with the length of the fibre. At a certain distance from the fibre input the arc closes up into a circle, then the second revolution occurs, etc. If we complete the complex plane with the third coordinate displaying the wavelength, then the set of points will be represented by a helix (Fig. 2), the number of helix turns (and, respectively, its length) growing with the length of the fibre z. In the case of small spectral width ($\Delta\lambda \ll \lambda_0$) the rotation frequency Ω linearly depends on the wavelength λ:

$$\Omega(\lambda) = (2\xi+\gamma)\left(1+\frac{\sigma_0^2\lambda_0^2}{\lambda^2}\right)^{1/2}$$
$$\approx \frac{2\xi+\gamma}{\sqrt{\sigma_0^2+1}}\left(2\sigma_0^2+1-\sigma_0^2\frac{\lambda}{\lambda_0}\right), \tag{13}$$

where $\sigma_0 = L_\mathrm{tw}/2L_\mathrm{b}(\lambda_0)$ is the parameter of the spun fibre at the centre wavelength λ_0.

The phase difference between the polarisation points at the boundary wavelengths of the spectrum is determined by the difference of their rotation frequencies $\Delta\Omega = \Omega(\lambda_0 + \Delta\lambda/2) - \Omega(\lambda_0 - \Delta\lambda/2)$. From here one can derive the dependence of the number of turns $K(z)$ on the distance:

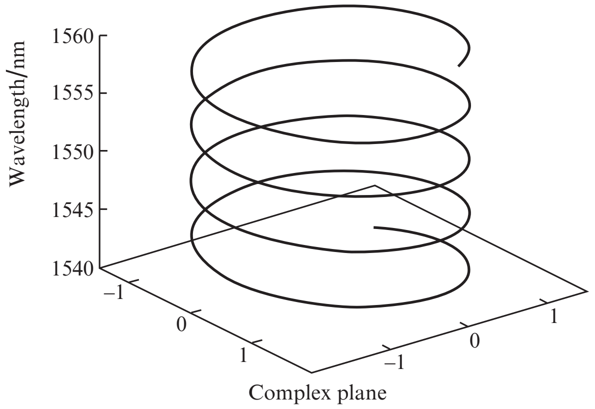

Figure 2. Set of PS points on the complex plane as a function of wavelength.

$$K(z) = \frac{\Delta\Omega}{2\pi} z = \frac{(2\xi + \gamma)\sigma_0^2}{2\pi\sqrt{\sigma_0^2 + 1}} \frac{\Delta\lambda}{\lambda_0} z. \quad (14)$$

The length of the spun fibre, at which the set of PS points of the spectral components of the propagating broadband radiation closes up into a circle, will be referred to as the coherence length $L_{\rm coh}$. Assuming that $K(L_{\rm coh}) = 1$, we get

$$L_{\rm coh} = \frac{2\pi}{2\xi + \gamma} \frac{\sqrt{\sigma_0^2 + 1}}{\sigma_0^2} \frac{\lambda_0}{\Delta\lambda}. \quad (15)$$

Therefore, the PS points of all spectral components of the broadband light, entering the fibre, after passing the distance $z > L_{\rm coh}$ along the fibre, become uniformly distributed along a single circle centred at zero and having the radius $|\chi_{\rm e}(0)|$ in the basis of the elliptical PS. For the radiation spectrum with $\lambda_0 = 1550$ nm and $\Delta\lambda = 20$ nm and the fibre with $L_{\rm b} = 1.7$ mm and $L_{\rm tw} = 2.68$ mm the coherence length amounts to $L_{\rm coh} = 21$ cm.

In the previous section it was shown that on the Poincare sphere the points, corresponding to the basis PS of the rotating coordinate frame, define the instantaneous axis that rotates together with the vector of built-up linear BR about the axis of its rotation with the frequency 2ξ. The set of PS points of the spectral components of the broadband radiation, equidistant from the basis points for the rotating PS coordinate system, is a circle on the Poincare sphere, the axis of which is the instantaneous axis (the UV axis in Fig. 3). The mean value of this PS distribution over the wavelengths, or the 'centre-of-mass' of the PS point set, lies on the instantaneous axis inside the sphere at a certain distance $OP = \rho$ from its centre (the residual nonuniformity of the distribution being neglected). The ratio of this distance to the radius of the sphere $P = \rho/R$ equals the degree of polarisation [14] of light, the expression for which will be derived below.

When the ellipticity and the azimuth of the input PS are varied, the set of different circles, containing the PS points for different wavelengths, is a family of different concentric circles of the Poincare sphere, centred at the instantaneous axis. Therefore, the segment, connecting the points of intersection of the instantaneous axis UV with the Poincare sphere, is the set of mean values of the PS distributions, or the set of centres of these circles. All these mean states possess the similar ellipticity and azimuth; they differ by the degree of polarisation only.

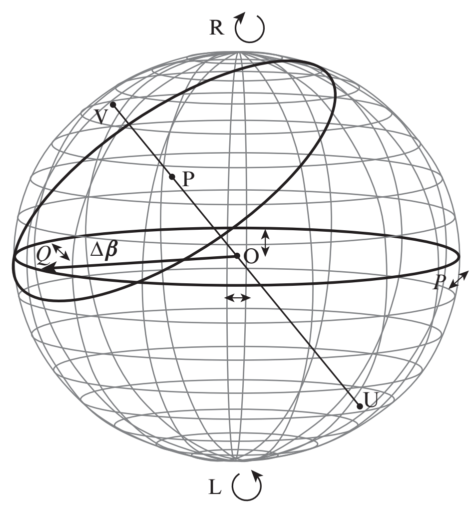

Figure 3. Computer modelling of the PS evolution for a spectral component of broadband light in a spun fibre.

Hence, it is possible to draw an important conclusion, namely, at $z > L_{\rm coh}$ the mean PS output from a segment of a spun fibre (within the orthogonal PS) does not depend on the input polarisation state, which determines only the degree of the output radiation polarisation. The mean PS has the ellipticity, determined by the fibre parameters, $e = \tan(\psi/2) = \sqrt{\sigma^2 + 1} - \sigma$ and the azimuth, coincident with the azimuth of one of the axes of the built-in linear BR. Let us refer this ellipticity as the eigenellipticity of the fibre with the given spun fibre parameter σ. The dependence of eigenellipticity on the beat length of the built-in linear BR is plotted in Fig. 4. We should emphasise that, strictly speaking, in spun fibres no true polarisation eigenstates conserved along the entire length of the fibre exist, since the azimuth of the mean PS rotates together with the axes of the built-in linear BR. Only the degree of polarisation P of the output radiation depends on the input polarisation state.

Let us find the dependence of the polarisation degree for the broadband light radiation on the input PS at $z > L_{\rm coh}$. The simple distribution of the PS on the Poincare sphere, lying on a circle (see Fig. 3), allows derivation of this dependence from the geometric drawing.

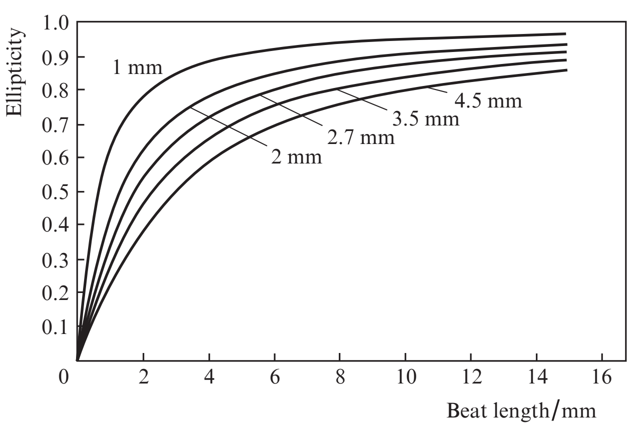

Figure 4. Dependence of eigenellipticity of the spun fibre on the beat length of the built-in birefringence at different helix pitches $L_{\rm tw} = 1$–4.5 mm.

Consider the section of the Poincare sphere in the laboratory coordinate system of the circular PS, containing the instantaneous axis UV and the vector of built-in linear BR $\Delta\boldsymbol{\beta}$ (Fig. 5). Let the input PS have the given ellipticity $e = \tan(\varepsilon) = \tan(\psi/2)$. On the Poincare sphere the set of points with fixed ellipticity and different azimuths forms a circle of equal latitude ψ (in Fig. 5 the projection of this circle onto the section is the segment $H_{max}H_{min}$). The plane of the circle, on which the output PS points with different wavelengths will lie, is tilted by the angle φ with respect to the equator plane. Both circles intersect at the input PS points, H_α being the projection of these crossing points. When the azimuth of the input PS θ is changed, the circles, on which the output PS points lie, will change, too. The projections of the circles, on which the PS points lie, onto the section, presented in Fig. 5, are segments, perpendicular to UV. The centres of the circles lie on the instantaneous axis UV. With variation of the input PS azimuth, the centre P will move from the point P_{max} to the point P_{min} (see Fig. 5), the degree of output polarisation P being calculated by division of ρ (the length of the segment OP) by the sphere radius [14]. After simple geometric calculations we get:

$$P(\psi,\theta) = \frac{\rho}{R} = \left| \frac{1 + \sigma\cot\psi\cos 2\theta}{\sqrt{(1+\sigma^2)(1+\cot^2\psi)}} \right|. \qquad (16)$$

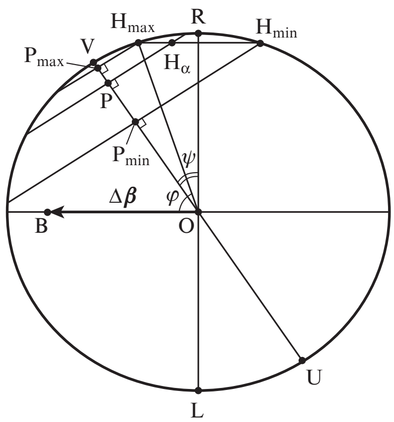

Figure 5. Section of a Poincare sphere in the laboratory coordinate system of the circular PS, containing the instantaneous axis UV.

The plot of the dependence of the degree of output polarisation on the azimuth of the input polarisation at different ellipticities for the spun fibre with the parameters $L_b = 1.7$ mm and $L_{tw} = 2.68$ mm is presented in Fig. 6.

Of particular interest are the dependences of P on the azimuth of the input polarisation for three types of polarisation – linear, circular and elliptical – with similar eigenellipticity, inherent in the considered spun fibre. In the case of linear input polarisation P depends on θ as the cosine modulus. When the axis of the input polarisation coincides with one of the axes of the built-in linear BR of the spun fibre at the input, the degree of the output polarisation has a maximum, the value of which is determined by the spun fibre parameter σ, and if the angle between the polarisation axis and the axes of the fibre amounts to 45°, then P decreases to zero. In the case of the circular input PS the degree of output polarisation, as expected, does not depend on the azimuth of the input PS and is determined by the parameter σ. Finally, if the radiation input into the spun fibre possesses ellipticity, equal to the

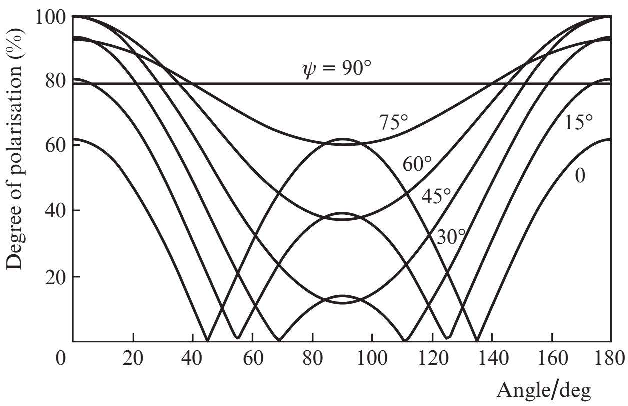

Figure 6. Dependence of the output radiation polarisation on the azimuth of the input polarisation at different latitudes of the input polarisation Ψ on the Poincare sphere for the spun fibre with the parameters $L_b = 1.7$ mm and $L_{tw} = 2.68$ mm.

eigenellipticity of the fibre, and the azimuth, coincident with that of one of the axes of the built-in linear BR at the input, then the degree of polarisation P remains equal to 100%, i.e., the degree of polarisation of light remains constant in the course of propagation along the fibre. In Fig. 5 this situation corresponds to the case, when the circle, on which the set of the PS points with different wavelengths lie, degenerates into a single point on the Poincare sphere.

3. Experiment

3.1. Measuring the helix pitch of the spun fibre

In Section 2.3 it was shown that the broadband light in a spun fibre propagates with a definite mean ellipticity, and the azimuth of the mean ellipse of polarisation θ grows along the fibre with the frequency of rotation of the built-in linear BR axes. This fact offers an opportunity to determine the helix pitch of the built-in linear BR using the chipping method, i.e., measuring the azimuth θ before and after chipping a segment of a fibre with the length L. In this case the helix pitch is $L_{tw} = 2\pi L/\Delta\theta$.

The schematic diagram of the experiment is presented in Fig. 7. The linearly polarised radiation with the spectral width 20 nm and the centre wavelength 1550 nm was introduced into the studied segment of microstructure spun fibre with the length 15 m and the calculated pitch of the helical structure 3 mm. The azimuths of the mean PS before and after chipping a small segment of the fibre were measured using a rotating analyser.

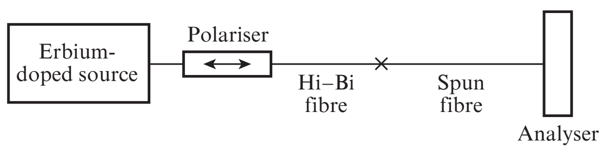

Figure 7. Schematic diagram of measuring the pitch of the spun fibre helix.

The results of a series of measurements, performed with the sample of microstructure spun fibre, are presented in Table 1, from which it follows that the mean pitch of the helix is $L_{tw} = 2.68$ mm.

Table 1. The results of measurements of the pitch of the spun fibre helix.

Number of measurement	Length of chipped fibre/μm	Angle of azimuth rotation/deg	Helix pitch/μm
1	1000±15	135±2	2670±80
2	800±15	106±2	2700±100
3	900±15	122±2	2660±90
4	460±15	63±2	2640±170
5	560±15	74±2	2740±140
6	625±15	84±2	2680±130
7	590±15	79±2	2680±140

3.2. Measuring the dependences of the output polarisation degree upon the azimuth of input polarisation

The schematic diagram of the experiment is shown in Fig. 8. The erbium-doped fibre source with the operating wavelength 1550 nm and the spectral width 20 nm was used as a source of radiation. The radiation output from the polariser excited one of linearly polarised modes of the Hi–Bi fibre. The radiation with three different PSs was introduced by turn into the studied microstructure fibre: first, with linear and circular polarisation, and then with elliptical polarisation (with the ellipticity, equal to the eigenellipticity of the given Hi–Bi fibre). To provide the input of linearly polarised radiation into the spun fibre, the output end of the Hi–Bi fibre and the input end of the spun fibre were fixed in the device, intended for oriented splicing of fibres. The device allowed rotation of the output end of the Hi–Bi fibre around its axis, thus changing the azimuth of the input radiation PS with respect to the axes of the built-in linear BR at the input of the spun fibre. The degree of polarisation of the radiation at the output of the spun fibre was analysed with the polarisation meter, consisting of the rotating $\lambda/4$ plate and analyser [13]. In Fig. 9 the results of measuring the polarisation degree at different azimuths are denoted by squares, the dashed line is the theoretical curve, obtained using Eqn (16) at the latitude of the input PS on the Poincare sphere $\psi = 0$ and the parameter of spun fibre $\sigma =$ 0.79.

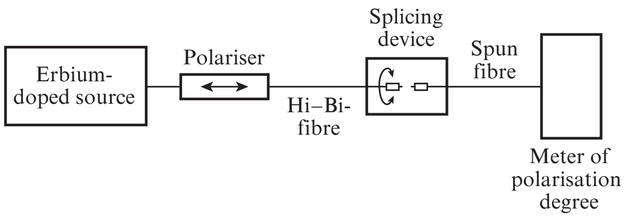

Figure 8. Schematic diagram of measuring the dependence of the output polarisation on the azimuth of the input polarisation.

To introduce the radiation with circular polarisation into the studied spun fibre, a fibre $\lambda/4$ retarder was spliced to the output of the Hi–Bi fibre. The attachment of the $\lambda/4$ retarder to the input of the spun fibre was also implemented using the device for oriented splicing of fibres. The measured dependence of the polarisation degree on the azimuth in Fig. 9 is shown by triangles; the dashed line shows the result of calculation using Eqn (16) for the latitude $\psi = 87°$ and the parameter $\sigma = 0.79$.

As seen from the Figure, the experimental results in the cases of linear and circular polarisation agree with the theory quite well. Therefore, to a certain degree of accuracy one can

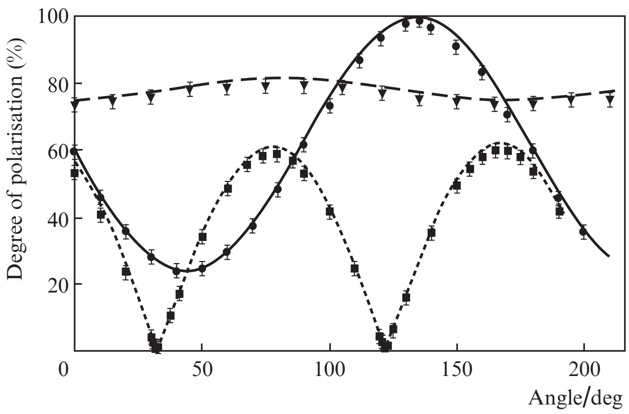

Figure 9. Dependence of the output polarisation degree on the angle of axial rotation of the input fibre in the splicing device at different PSs of input radiation: linear polarisation (squares – experiment, dashed line – calculation), circular input polarisation (triangles – experiment, dashed line – calculation), elliptic input polarisation (circles – experiment, solid line – calculation).

assert that for this sample of fibre is $\sigma = 0.79$, and, respectively, the eigenellipticity latitude on the Poincare sphere is $\psi = 52°$. Taking into account the pitch of the helix, measured in Section 3.1, the beat length calculated using Eqn (11) is found to be $L_b = 1.7$ mm.

Of particular interest is the experiment, in which the studied microstructure spun fibre was excited by the radiation with the ellipticity, coincident with the eigenellipticity of the given fibre. For this aim the fibre $\lambda/4$ retarder was shortened so that its length became $L_s = (52°/90°)L_{\lambda/4} = 0.57L_{\lambda/4}$. In the present experiment the length of the fibre $\lambda/4$ retarder was $L_{\lambda/4} = 1.7$ mm, so the retarder was shortened by $0.43L_{\lambda/4} = 0.73$ mm, after which the degree of polarisation of the radiation, output from the spun fibre, was measured at different azimuths of the input radiation. In Fig. 9 the results of these measurements are denoted by circles, and the solid curve shows the theoretical results. It is seen that at a definite azimuth of the input polarisation with respect to the axes of the built-in linear BR of the spun fibre at the input the degree of polarisation of the output radiation approaches 100%, which corresponds to the case of propagation of broadband radiation without loss of the polarisation degree, considered above.

4. Conclusions

The evolution of the PS of broadband light upon its propagation in a spun fibre with high built-in linear BR is studied. The theoretical model, describing the parameters of the PS of the radiation output from a segment of a spun fibre for the arbitrary PS of light at the input, is developed. The model is based on the summation of contributions of monochromatic components, distributed within the spectral width of the input radiation. The analysis uses the formalism of differential Jones matrix and the representation of the PS of light on the Poincare sphere. It is shown that when the propagation length exceeds some critical value (the coherence length), the mean PS of the polarisation distribution of the spectral components of the broadband light at the output of spun fibre segments (within the orthogonal PS) does not depend on the state of input polarisation. The mean PS has the ellipticity determined by the fibre parameters (mentioned as eigenellipticity) and the azimuth, coincident with the azimuth of one of the built-in linear BR axes. In this case only the degree of polarisation of the output radiation depends on the input polarisation state. The conditions of excitation are found, under which the degree of polarisation keeps constant and equal to 100% along the fibre. The criterion is found defining the minimal length of a spun fibre segment, for which the presentation of the output radiation PS described above is valid. This length (the coherence length) is determined by the spectral bandwidth of the radiation and the spun fibre parameters. Theoretical results are confirmed by experimental measurements.

References

1. Laming R.I., Payne D.N. *J. Lightwave Technol.*, **7**, 2084 (1989).
2. Frosio G., Dancliker R. *Appl. Opt.*, **33**, 6111 (1994).
3. Blake J., Williams W., Glasov C., Bergh R., Fetting K., Hadley E., Sanders G. *Proc. 2nd EPRI Opt. Sensors Systems Workshop* (Atlanta, 2000).
4. Starostin N.I., Ryabko M.V., Chamorovskii Yu.K., et al. *Key Eng. Mater.*, **437**, 314 (2010).
5. Gubin V.P., Isaev V.A., Morshnev S.K., et al. *Kvantovaya Elektron.*, **36**, 287 (2006) [*Quantum Electron.*, **36**, 287 (2006)].
6. Chamorovsky Yu.K., Starostin N.I., Ryabko M.V., et al. *Opt. Commun.*, **282**, 4618 (2009).
7. Morshnev S.K., Gubin V.P., Vorobyov I.L., et al. *Kvantovaya Elektron.*, **39**, 287 (2009) [*Quantum Electron.*, **39**, 287 (2009)].
8. Gubin V.P., Morshnev S.K., Starostin N.I., et al. *Kvantovaya Elektron.*, **41**, 815 (2011) [*Quantum Electron.*, **41**, 815 (2011)].
9. Michie A., Canning J., Bassett I., et al. *Opt. Express*, **15**, 1811 (2007).
10. Chamorovskii Yu.K., Starostin N.I., Morshnev S.K., et al. *Kvantovaya Elektron.*, **39**, 1074 (2009) [*Quantum Electron.*, **39**, 1074 (2009)].
11. Polynkin P., Blake J. *J. Lightwave Technol.*, **23**, 3815 (2005).
12. Malykin G.B., Pozdnyakova V.I., Shereshevskii I.A. *Opt. Spektrosk.*, **83**, 843 (1997) [*Opt. Spectrosc.*, **83**, 780 (1997)].
13. Gubin V.P., Morshnev S.K., Starostin N.I., et al. *Radiotekh. Elektron.*, **53**, 971 (2008) [*J. Commun. Technol. Electron.*, **53** (8), 918 (2008)].
14. Azzam R.M.A., Bashara N.M. *Ellipsometry and Polarised Light* (Amsterdam – New York – Oxford: North-Holland Publ. Comp., 1977).
15. Rashleigh S.C. *J. Lightwave Technol.*, **1**, 312 (1983).
16. Gorshkov M.M. *Ellipsometriya* (Ellipsometry) (Moscow: Sov. Radio, 1974).
17. Rose A.H., Etzel S.M., Wang C.M. *J. Lightwave Technol.*, **15**, 803 (1997).